TIME-DOMAIN MODELS OF MARINE SURFACE VESSELS BASED ON SEAKEEPING COMPUTATIONS

Tristan Perez [*] **Thor I. Fossen** [*,**]

[*] *Centre for Ships and Ocean Structures (CeSOS)*
[**] *Department of Engineering Cybernetics*

Norwegian University of Science and Technology (NTNU), Trondheim, NORWAY.

Abstract: This paper discusses the use of seakeeping data (frequency-domain data) for obtaining preliminary time-domain models for simulation and control design with application to surface vessels. Modelling is discussed according to both the theories of manoeuvring and seakeeping, with emphasis on the latter. The linear frequency-domain model commonly used in hydrodynamics is revisited together with its equivalent time-domain counterpart (Cummins Equation) and the computation of its parameters using standard hydrodynamic codes and system identification.

Keywords: Marine systems, models.

1. MOTIVATION

The number of applications of model-based guidance, monitoring, and control of surface marine vessels has increased significantly during the last 20 years in the shipping and offshore industries. This has enabled operations in higher sea states and contributed to higher economy and reliability of marine operations. These control applications span over guidance and control systems for course and tracking autopilots, dynamic positioning, thruster assisted position mooring, ride control, roll stabilization, heave compensation, and formation control.

Despite the large number of applications of model-based control to marine systems, one of the main problems the designer faces is that of obtaining reliable models for computer simulations, control design and control testing. There are two main factors that have impact on this:

(1) The dynamic response of the vessel changes due to changes in the vessel operational conditions (VOCs). Therefore, models spanning over different conditions are necessary.
(2) There is, usually limited access to experimental data. Experiments on either full scale and scaled models can be very costly; and therefore, they are only performed for certain VOCs.

To discuss this further, let us define the *vessel operational condition* (VOC) as a triplet of attributes (Perez *et al.*, 2006):

$$VOC = \langle use\,mode,\ environment,\ vessel\,cond \rangle,$$

where

- *use mode* indicates the current task: station keeping, transit, tracking, etc.
- *environment* refers to the state of the environment: waves, current, wind, and the water depth.

- *vessel cond* refers to the condition of the vessel: speed, loading (mass distribution), available resources (power, communications, navigation systems, actuators, *etc*).

During a particular operation or mission, a vessel can move through different VOCs. The VOC has a significant influence on the dynamic response of the vessel and thus the model. To obtain such models, one can follow different paths: *experimental methods*, *computational methods*, or a combination of both.

Experimental methods can be based on scaled models or on the full scale ship for specific VOC. In some fortunate cases, these tests are performed and a parametric model for the dynamic response of the vessel may be obtained, which can be used for preliminary control design. This, however, is not the usual case: most ship owners do not have such parameters for all the ships in their fleets, and if they have any, they may be valid only in restrictive VOCs.

The prediction of ship responses and loads using hydrodynamic computations have become an important tool in the design of marine structures, and high quality of the predictions is obtained in most applications (Beck and Reed, 2001; Faltinsen, 2005). These methods are nowadays available as commercial seakeeping codes, which provide the frequency responses of the vessel from the waves to the wave-induced forces, and from the forces to motion. Because the data computed by hydrodynamic codes are, often, in the frequency domain, processing is needed in order to obtain models for time-domain simulations and control design. Once this is done, one can have a *preliminary* model. Here, we say preliminary because the model obtained is often based on potential theory, which does not incorporate viscous effects; that is, it leaves out part of the model for which either experimental data, or engineering judgement is necessary. In this paper, we discuss the use of data from hydrodynamic codes for obtaining preliminary time-domain models for simulation and control design applications for surface vessels.

2. VESSEL DYNAMICS AND MOTION CONTROL

The study of ship dynamics has traditionally been separated into two main areas:

- *Manoeuvring (steering and manoeuvrability)*,
- *Seakeeping*.

For a variety of reasons these areas have evolved in different ways and they are still separated to date. As discussed by Abkowitz (1964), Norrbin (1970), Clarke (2003), and Faltinsen (2005), **Manoeuvring** refers to studies that consider ship motion in the horizontal plane (surge-sway-yaw, or surge-sway-yaw-roll) due to the action of control devices (propulsion systems and control surfaces) in the absence of wave-excitation (calm water). These studies are aimed at assessing the ship capabilities to turn by the action of the control devices. The mathematical models obtained from manoeuvring studies are used in ship simulators, and to determine the ship's directional stability and design and testing of tracking and course keeping autopilots.

Seakeeping, on the other hand, refers to the study of motion when there is wave excitation and while the vessel keeps its course and its speed constant (which includes the case of zero speed). In seakeeping, the control surfaces may be used to reduce the motion induced by the waves—*motion damping and stabilisation*. Seakeeping studies aim at quantifying the vessel motion due to wave action. This studies often consider motion in 6 degrees of freedom (DOF). The models obtained from seakeeping studies are used to evaluate performance indices that depend on statistics of the motion—see, for example, Lloyd (1998).

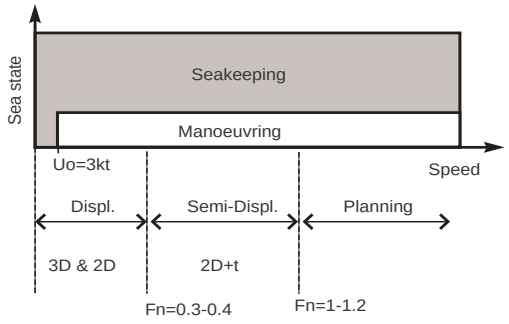

Fig. 1. Range of speed and environment covered in manoeuvering and seakeeping.

Figure 1 shows a representation of the range of speed and environment covered in the theories of seakeeping and manoeuvring. This figure also shows the vessel behaviour according the different speed regimes, which are refined in terms of the Froude number: $Fn = U/\sqrt{Lg}$ with L being the length of the vessel. For Fn <0.3 the hull is supported mostly by hydrostatic pressure and the vessels operating in this regime are called *displacement vessels*. For 0.4< Fn <1 the hydrodynamic pressure become important and lift effects start to appear. Vessels operating in these regimes are called *semi-displacement vessels*. For 1> Fn there is a strong flow separation and aerodynamics also play an important role. Vessel operating in these regimes are called *planning vessels*. The separation into these speed regimes has bearing on the theories used in hydrodynamics to compute estimates of the wave induced forces and the motion of the vessel. For instance for zero forward

speed 3D codes [1] are available and this is the standard in offshore applications. For vessels with forward speed the use of 2D codes (strip theory) is commonly use for Fn <3. For 4< Fn <1, 2D+t codes are commonly used. For further details see Faltinsen (2005).

When the two areas of seakeeping and manoeuvring are combined we have studies of *manoeuvring in seaway*. Although manoeuvring and seakeeping are concerned with the same issues: study of motion, stability and control, the separation allows making different assumptions that simplify the study in each case. The main hypothesis upon which these theories are based can be summarized in the following:

Manoeuvring

- Calm water environment.
- Motion description using body-fixed coordinates.
- Only horizontal plane motion (+roll).
- Motion is considered within a nonlinear framework.
- Motion produced by the forces generated due propulsion systems and control surfaces.
- Study of motion during manoeuvres at forward speed.
- Mathematical time-domain models are obtained from data of scaled model tests, in which the models are forced to move while motion and forces are logged. The experiments are normally performed at different forward speeds.

Seakeeping

- Seaway environment.
- Motion description using equilibrium coordinates.
- Motion is produced by wave-induced forces in 6 DOF, and it is considered within a linear framework.
- Zero and forward speed.
- Motion is generally studied while the vessel keeps a constant (average) course and speed, and the waves induce perturbations with respect to an equilibrium state.
- Due to the linearity assumption, the problem can be studied in the frequency-domain, and the ship frequency response functions are generally obtained using numerical computation methods, which have been validated against experimental data.

When it comes to the design end evaluation of different marine control systems the ultimate goal would be to have models that span over these two areas. That is for different speeds and sea states.

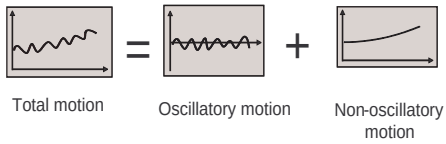

Fig. 2. Ship motion components.

The task of a ship motion control system consists of making the ship to follow a desired trajectory, defined in terms of the ships position, velocity, and acceleration. It is common to separate the motion into two different components, as illustrated in Figure 2. The non-oscillatory component of motion is the result of non-oscillatory slowly-varying forces, while the oscillatory motion is induced by wave loads—which are the result of oscillatory variations of pressure on the hull. Due to this separation we can divide different control problems into three main categories:

(1) *Control only the non-oscillatory motion.*
(2) *Control only the oscillatory motion.*
(3) *Control the total motion.*

The first category includes problems course and tracking autopilots, dynamic positioning and thruster assisted position mooring in lower sea states. The second category include problems of ride control systems of high speed vessels (for roll and pitch damping), roll stabilization, and heave compensation of tension offshore structures. The third category is characteristic of autopilots with rudder roll stabilization, dynamic positioning and thruster assisted position mooring in extreme seas.

These different control problems result in different uses of the available models from the theories of manoeuvring and seakeeping. As discussed in Perez *et al.* (2004) and Perez (2005), two main approaches are commonly used to modeling of marine vessels for control system design:

(1) *Motion superposition models based on manoeuvring and seakeeping models*,
(2) *Force superposition models based on seakeeping data with added viscous effects.*

The motion superposition type of model is represented by the block diagram shown in Figure 3(a). In these models, a manoeuvring model is used to describe the relationship between the control action and the motion induced by this control action and a seakeeping model is used to describe the motion due to the waves. This type of model presents two shortcomings. The first one is that the model may not be used for multi-body system interactions. This requires energy exchange, *i.e.,* it requires elements with common forces and speeds,

[1] The acronym xD stands for x-dimensional. This reflects the fluid motion assumptions made in the underlying theory.

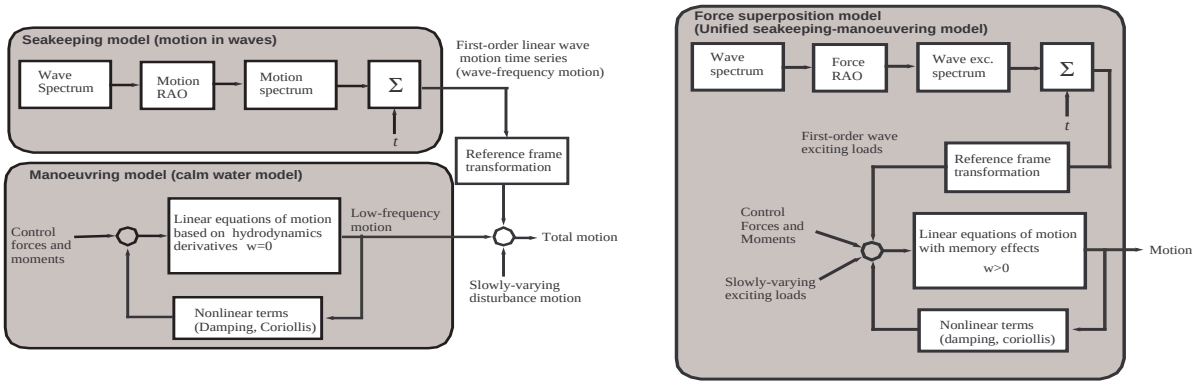

Fig. 3. Models of marine vessels for control. (a)-motion superposition model; (b)-force superposition or unified model.

and this is not captured by a models that uses motion as a disturbance. The second shortcoming is that the manoeuvring part does not incorporate fluid-memory effects associated with the waves radiated as a consequence of the motion of the ship.

An alternative approach consists of using a model with force superposition rather than motion superposition, as illustrated in Figure 3(b). In this model, the wave to force frequency responses (or force RAO) are combined with the sea spectrum to give the wave-excitation forces. Also, a time-domain representation is used for the fluid memory effects associated with the waves radiated from the ship. In this time-domain representation, the radiation forces are computed using both the wave- and control-induced motion instead of only the wave-induced motion as in the model shown in Figure 3(a).

The model shown in Figure 3(b) is well known in marine environment and it is part of the state of art time-domain simulation of wave to structure interaction. However, its use in marine control system design has not yet been widely adopted.

In this paper, we will be concentrating on the second type of model, and discuss how hydrodynamic computations can be used to obtain parameters of such models. For a thorough discussion of manoeuvring models the reader is referred to Abkowitz (1964), Norrbin (1970), Clarke (2003), and references therein.

3. KINEMATICS OF SHIP MOTION

3.1 Unified coordinates

To describe the position and orientation of a ship the following orthonormal right-hand-sided reference frames are commonly used:

- Noth-East-Down (n-frame),
- Body-fixed (b-frame),

These frames, which are indicated in Figure 4, have specific uses. The n-frame is the local geographical frame used to define the position of the vessel on the earth, and the direction of wind and current. The b-frame is the frame to which all the velocity and acceleration measurements taken on board are referred. This frame is used to formulate the equations of motion—for further details see, for example, Fossen (2002) and Perez (2005).

The *position* of a vessel is defined by the coordinates of the origin of the b-frame relative to the n-frame:

$$\mathbf{r}^n_{no_b} = \begin{bmatrix} N & E & D \end{bmatrix}^T,$$

where N denotes the *North* position, E denotes the *East* position, and D denotes the *Down* position. The lower script no_b indicates that the vector describes the position of the point o_b with respect to the n-frame, while the upper scrip indicates in which reference frame the vector is expressed. This is illustrated in Figure 4, which also shows the ship trajectory and the linear-velocity vector. $\dot{\mathbf{r}}^n_{no_b}$.

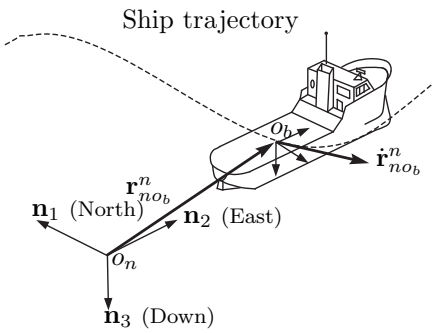

Fig. 4. Ship position and velocity vectors.

The *attitude* (or *orientation*) of a vessel is defined by the orientation of the b-frame relative to the

n-frame. This is given by the *three* consecutive rotations about the main axes that take the n-frame into the b-frame. These rotations can be performed in a different order (there are 12 different ways of doing this), and each triplet of angles rotated are called a set of *Euler angles*. The most standard set of Euler angles are *yaw*, *pitch* and *roll* (SNAME, 1950). The vector of roll, pitch and yaw that take the n-frame into the orientation of the b-frame will be denoted by

$$\boldsymbol{\Theta}_{nb} = \begin{bmatrix} \phi & \theta & \psi \end{bmatrix}^T. \tag{1}$$

Following the notation of Fossen (1994), the *generalised position vector* (position and orientation) is defined as

$$\boldsymbol{\eta} \triangleq \begin{bmatrix} \mathbf{r}^n_{no_b} \\ \boldsymbol{\Theta}_{nb} \end{bmatrix} = [N, E, D, \phi, \theta, \psi]^T. \tag{2}$$

The linear and angular velocities of the ship are more conveniently expressed in the b-frame—this simplifies the equations of motion and is consistent with the measurements taken onboard (Fossen, 1994; Fossen, 2002). The *generalised velocity vector* (linear-angular velocity vector) given in the b-frame is defined as:

$$\boldsymbol{\nu} \triangleq \begin{bmatrix} \mathbf{v}^b_{no_b} \\ \boldsymbol{\omega}^b_{nb} \end{bmatrix} = [u, v, w, p, q, r]^T, \tag{3}$$

where according to the adopted notation:

- $\mathbf{v}^b_{no_b} = [u, v, w]^T$ is the linear velocity of the point o_b with respect to the n-frame expressed in the b-frame. Thus, $\mathbf{v}^b_{no_b}$ results from expressing $\dot{\mathbf{r}}^n_{no_b}$ in the b-frame—see Figure 4.
- $\boldsymbol{\omega}^b_{nb} = [p, q, r]^T$ is the angular velocity of the b-frame with respect to the n-frame expressed in the frame b.

We call the variables $\boldsymbol{\eta}$ and $\boldsymbol{\nu}$ *unified coordinates*, because they describe the motion of the vessel in any vessel operational condition. Note that these coordinates are the ones used in manoeuvring theory.

A kinematic transformation provide the link between the body-fixed velocities $\boldsymbol{\nu}$ and time derivative of the vessel trajectory $\dot{\boldsymbol{\eta}}$:

$$\dot{\boldsymbol{\eta}} = \mathbf{J}^n_b(\boldsymbol{\Theta}_{nb})\, \boldsymbol{\nu}, \tag{4}$$

where

$$\mathbf{J}^n_b(\boldsymbol{\Theta}_{nb}) \triangleq \begin{bmatrix} \mathbf{R}^n_b(\boldsymbol{\Theta}_{nb}) & \mathbf{0}_{3\times 3} \\ \mathbf{0}_{3\times 3} & \mathbf{T}_{\boldsymbol{\Theta}}(\boldsymbol{\Theta}_{nb}) \end{bmatrix}, \tag{5}$$

in which the linear velocity transformations are given in terms of the *rotation* matrix:

$$\mathbf{R}^n_b(\boldsymbol{\Theta}_{nb}) = \begin{bmatrix} c\psi c\theta & -s\psi c\phi + c\psi s\theta s\phi & s\psi s\phi + c\psi c\phi s\theta \\ s\psi c\theta & c\psi c\phi + s\phi s\theta s\psi & -c\psi s\phi + s\psi c\phi s\theta \\ -s\theta & c\theta s\phi & c\theta c\phi \end{bmatrix}, \tag{6}$$

and the angular velocity transformation is given in terms of the matrix

$$\mathbf{T}_{\boldsymbol{\Theta}}(\boldsymbol{\Theta}_{nb}) = \begin{bmatrix} 1 & s\phi t\theta & c\phi t\theta \\ 0 & c\phi & -s\phi \\ 0 & s\phi/c\theta & c\phi/c\theta \end{bmatrix}, \qquad c\theta \neq 0,$$
$$\mathbf{T}_{\boldsymbol{\Theta}}(\boldsymbol{\Theta}_{nb})^{-1} = \begin{bmatrix} 1 & 0 & -s\theta \\ 0 & c\phi & c\theta s\phi \\ 0 & -s\phi & c\phi c\theta \end{bmatrix}, \tag{7}$$

where $s \equiv \sin(\cdot)$ and $c \equiv \cos(\cdot)$. The rotation matrix (6) belongs to the *special orthogonal group of order 3*, $SO(3)$. Thus, $(\mathbf{R}^n_b)^{-1} = (\mathbf{R}^n_b)^T = \mathbf{R}^b_n$. Note that the transformation $\mathbf{T}_{\boldsymbol{\Theta}}(\boldsymbol{\Theta}_{nb})$ is not orthogonal; therefore, $\mathbf{T}_{\boldsymbol{\Theta}}(\boldsymbol{\Theta}_{nb})^T \neq \mathbf{T}_{\boldsymbol{\Theta}}(\boldsymbol{\Theta}_{nb})^{-1}$. For further details on the derivations of these transformations see, for example, Fossen (2002).

3.2 Seakeeping coordinates

In seakeeping theory *the study ship motion is performed under the assumption that it can be described as the superposition of an equilibrium state of motion plus perturbations.* The equilibrium is determined by a constant course and speed, and the perturbations are zero-mean oscillatory components induced by first-order wave excitation. Note that the case of zero vessel speed is also contemplated as an equilibrium of motion.

Due to this, the motion is often described using an *equilibrium or hydrodynamic reference frame: h-frame.* This frame is not-fixed to the vessel; it is fixed to the equilibrium state. That is, in the absence of wave excitation, the origin o_h coincides with the location of a point s in the ship. Under the action of the waves, the hull is disturbed from its equilibrium and the point s oscillates, with respect to its equilibrium position. This is illustrated in Figure 5.

The h-frame is considered *inertial*; and therefore, its orientation with respect to the n-frame is fixed (or must vary very slowly)—as we shall see, this assumption results in linear equations of motion described in the h-frame. The velocity of the h-frame with respect to the n-frame is

$$\bar{\mathbf{v}}^n_{no_h} = \begin{bmatrix} U\cos\overline{\psi},\ U\sin\overline{\psi},\ 0 \end{bmatrix}^T, \tag{8}$$

where U is the average forward velocity of the vessel, and $\overline{\psi}$ the equilibrium heading—see Figure 5.

The *seakeeping or perturbation coordinates* are then defined as

$$\boldsymbol{\xi} \triangleq \begin{bmatrix} \mathbf{r}^h_{hs} \\ \boldsymbol{\Theta}_{hs} \end{bmatrix} = [\xi_1, \xi_2, \xi_3, \xi_4, \xi_5, \xi_6]^T. \tag{9}$$

The first three coordinates describe the position of the point s with respect to the h-frame, and the last three coordinates are the Euler angles

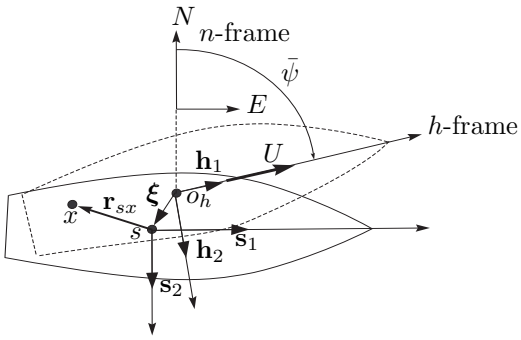

Fig. 5. Seakeeping coordinates. In absence of wave excitation, the frames h- and s-frame coincide.

that take the h-frame into the orientation of the s-frame $(s, \mathbf{s}_1, \mathbf{s}_2, \mathbf{s}_3)$ fixed to the body at at the point s—see Figure 5.

The linear coordinates of (9) are referred to as ξ_1—surge perturbation, ξ_2—sway perturbation, and ξ_3—heave perturbation. If the axes of the s-frame are parallel to those of the b-frame used in manoeuvring theory, we can then write

$$\boldsymbol{\Theta}_{hs} = \boldsymbol{\Theta}_{hb} \triangleq \begin{bmatrix} \xi_4 \\ \xi_5 \\ \xi_6 \end{bmatrix} = \begin{bmatrix} \phi - \overline{\phi} \\ \theta - \overline{\theta} \\ \psi - \overline{\psi} \end{bmatrix}, \qquad (10)$$

where $\overline{\phi}, \overline{\theta}, \overline{\psi}$ are the equilibrium angles; that is $\boldsymbol{\Theta}_{nh} = [\overline{\phi}, \overline{\theta}, \overline{\psi}]^T$. Normally we consider $\overline{\phi} = \overline{\theta} = 0$.

The perturbation angles are referred to as ξ_4—roll perturbation, ξ_5—pitch perturbation, and ξ_6—yaw perturbation. The perturbation coordinates can be used to describe the oscillatory position of any point of interest with respect to h-frame.

Table 1 summarizes the notation for the unified and seakeeping coordinates.

Table 1. Summary of nomenclature used for unified and seakeeping coordinates.

Var.	Name	Definition frame
N	North position	n-frame
E	East position	n-frame
D	Down position	n-frame
ϕ	Roll angle	Euler angle $(n \to b)$
θ	Pitch angle	Euler angle $(n \to b)$
ψ	Heading or yaw	Euler angle $(n \to b)$
u	Surge velocity	b-frame (w.r.t n-frame)
v	Sway velocity	b-frame (w.r.t n-frame)
w	Heave velocity	b-frame (w.r.t n-frame)
p	Roll rate	b-frame (w.r.t n-frame)
q	Pitch rate	b-frame (w.r.t n-frame)
r	Yaw rate	b-frame (w.r.t n-frame)
ξ_1	Surge perturbation	h-frame
ξ_2	Sway perturbation	h-frame
ξ_3	Heave perturbation	h-frame
ξ_4	Roll perturbation	Euler angle $(h \to b)$
ξ_5	Pitch perturbation	Euler angle $(h \to b)$
ξ_6	Yaw perturbation	Euler angle $(h \to b)$

The seakeeping coordinates are valid only for a very specific set of conditions that render the h-frame inertial, *i.e.*, constant speed and slowly-varying changes in heading. If we seek a set of coordinates to describe ship motion for control models, which are valid for all the vessel operational conditions, we need to use the *unified coordinates* $\boldsymbol{\eta}$ and $\boldsymbol{\nu}$ defined in (2) and (3). Despite the restrictions of the seakeeping coordinates, they are very important because most of the theory of ship hydrodynamics and the codes used to compute hydrodynamic data (motion and loads) use these coordinates. The kinematic transformation between seakeeping and unified is presented in the Appendix.

4. EQUATIONS OF MOTION: KINETICS

If we consider the equations of motion in the h-frame, we can write

$$\mathbf{M}^h_{RB} \ddot{\boldsymbol{\xi}} = \boldsymbol{\tau}^h, \qquad (11)$$

where $\mathbf{M}^h_{RB}$ is the generalized mass matrix. For simplicity of the representation, the following approximation is generally made:

$$\mathbf{M}^h_{RB} \approx \mathbf{M}^s_{RB} \triangleq \begin{bmatrix} m\mathbf{I}_{3\times 3} & -m\mathbf{S}(\mathbf{r}^s_{sg}) \\ m\mathbf{S}(\mathbf{r}^s_{sg}) & \mathbf{I}^s \end{bmatrix}, \qquad (12)$$

where $\mathbf{r}^s_{sg}$ indicates the position of the center of gravity with respect to the s-frame, and $\mathbf{I}^s$ is the inertia tensor about o_s. The matrix $\mathbf{S}$ is a skew-symmetric matrix given in the Appendix—see (A.2). This approximation is valid if the vessel motions are not extreme. This simplifies the formulation because the inertia components of the matrix $\mathbf{M}^h_{RB}$ are then independent of $\boldsymbol{\xi}$—see Fossen (2002).

The main advantage of formulating the equations of motion in terms of the seakeeping coordinates is the linearity of (11). The terms on the right-hand side of (11) represent the resultant of the different forces and moments acting on the vessel in the 6 DOF:

$$\boldsymbol{\tau}^h = [\tau^h_1, \tau^h_2, \tau^h_3, \tau^h_4, \tau^h_5, \tau^h_6]^T, \qquad (13)$$

The vector (13) can be separated into two components according to their originating effects:

$$\boldsymbol{\tau}^h = \boldsymbol{\tau}^h_{\text{hyd}} + \boldsymbol{\tau}^h_{\text{ctr}},$$

where $\boldsymbol{\tau}^h_{\text{hyd}}$-*hydrodynamic* forces, and $\boldsymbol{\tau}^h_{\text{ctr}}$-*control* and other external forces.

The *hydrodynamic forces* can be further divided into

$$\boldsymbol{\tau}_{\text{hyd}} = \boldsymbol{\tau}_{\text{rad}} + \boldsymbol{\tau}_{\text{visc}} + \boldsymbol{\tau}_{\text{hs}} + \boldsymbol{\tau}_{\text{wex}},$$

The *radiation forces* $\boldsymbol{\tau}_{\text{rad}}$ reflects the change of momentum in the fluid due to the motion of the vessel. These forces have a conservative part proportional to the vessel accelerations and non-conservative part proportional to the vessel velocities due the energy carried away by waves

radiating from the vessel due to its motion. Also, these forces incorporate *fluid memory effects*; and therefore there are further dynamics involved:

$$\boldsymbol{\tau}_{\text{rad}} = \boldsymbol{\tau}_{\text{rad}}(\dot{\boldsymbol{\nu}}, \boldsymbol{\nu}, \boldsymbol{\mu})$$

where $\boldsymbol{\mu}$ represents the fluid memory effects and has the following state-space representation:

$$\begin{aligned} \dot{\mathbf{x}} &= \mathbf{A}_r \mathbf{x} + \mathbf{B}_r \dot{\boldsymbol{\xi}} \\ \boldsymbol{\mu} &= \mathbf{C}_r \mathbf{x}. \end{aligned} \tag{14}$$

The states $\mathbf{x}$ in (14) reflect the fact that once the vessel changes the momentum of the fluid, this will affect the forces in the future. In other words, the radiation forces at a particular time depend on the history of the velocity of the vessel up to the present time. The dimension of $\mathbf{x}$ and the matrices $\mathbf{A}_r$, $\mathbf{B}_r$ and $\mathbf{C}_r$ will be specified later.

The *viscous forces* $\boldsymbol{\tau}_{\text{visc}}$ are non-conservative forces due to viscous phenomena (skin friction and flow separation). These forces appear as a consequence of the kinetic energy of the vessel being transferred to the fluid.

The pressure supporting the vessel, can be separated into hydrostatic and hydrodynamic. The hydrostatic pressure gives the buoyancy force which is proportional to the displaced volume. Thus, the *hydrostatic forces* $\boldsymbol{\tau}_{\text{hs}}$ the are restoring forces due to gravity buoyancy that tend to bring the vessel back its upright equilibrium position. The *wave excitation forces* $\boldsymbol{\tau}_{\text{wex}}$ arise due to changes in pressure due to waves. These have one component that varies linearly with the wave elevation and another that varies nonlinearly:

$$\boldsymbol{\tau}_{\text{wex}} = \boldsymbol{\tau}_{wl} + \boldsymbol{\tau}_{wnl}$$

The linear forces $\boldsymbol{\tau}_{wl}$ are oscillatory forces with a zero mean; these forces are called *first-order wave forces*—Froude-Kriloff and diffraction forces (Faltinsen, 1990). The energy of these forces is distributed at the same frequencies as the wave elevation seen from the moving ship (encounter frequencies). The non-linear components $\boldsymbol{\tau}_{wnl}$ give rise to a non-oscillatory forces: *mean wave drift forces*, and also to oscillatory forces which have energy at frequencies that are both lower and higher than the range of first-order wave loads. The components at lower frequencies are called *slow wave drift loads*, and together with the mean wave drift and the first-order loads constitute the main disturbances for ship motion control. The high frequency forces are usually of no concern for ship motion control, but can produce oscillation in the structure of the vessel—this effect is known as springing. For further details on wave loads see Faltinsen (1990) and Faltinsen (2005).

5. THE FREQUENCY-DOMAIN MODEL

If we consider a vessel sailing at a forward speed U, and also consider sinusoidal motion in the different DOF at the frequency ω, it can be show using potential theory that the steady-state radiation forces in the h-frame can be represented as

$$\boldsymbol{\tau}^h_{\text{rad}} = -\mathbf{A}^h(\omega, U)\ddot{\boldsymbol{\xi}} - \mathbf{B}^h(\omega, U)\dot{\boldsymbol{\xi}}, \tag{15}$$

That is, we consider the motion in the each DOF to be harmonic with the same frequency and amplitudes and phases $\bar{\xi}_i$ and $varepsilon_i$, for $i = 1, ..., 6$—see Faltinsen (1990) and Newman (1977) for further details. Note that ω will denotes the encounter frequency.

The matrix $\mathbf{A}^h(\omega, U)$ is the *added mass matrix*, and the first term in (15) describes forces that are the consequence of the change in momentum of the fluid due to the motion of the vessel. The matrix $\mathbf{B}^h(\omega, U)$ is the *potential damping matrix*, and the second term in (15) describes dissipative forces due to the energy carries in the waves generated by the vessel.

Let us also consider a linear approximation of the hydrostatic forces:

$$\boldsymbol{\tau}^h_{\text{hs}} = -\mathbf{g}^h(\boldsymbol{\xi}) \approx -\mathbf{G}^h_s \boldsymbol{\xi}. \tag{16}$$

The only non-zero linear restoring coefficients are (Faltinsen, 1990)

$$\begin{aligned} G^h_{s33} &= \rho g A_{WP} \\ G^h_{s35} &= C^h_{53} = -\rho g \iint_{A_{WP}} x^h \, ds \\ G^h_{s44} &= \rho g \nabla GMt, \quad G^h_{s55} = \rho g \nabla GMl, \end{aligned} \tag{17}$$

where A_{WP} is the water-plane area, ∇ is the displaced volume, and GMt and GMl are the transverse and longitudinal metacentric heights.

By substituting (17) and (15) into (11), we obtain the *frequency-domain equation of motion*:

$$[\mathbf{M}^h_{RB} + \mathbf{A}^h(\omega, U)]\ddot{\boldsymbol{\xi}} + \mathbf{B}^h(\omega, U)\dot{\boldsymbol{\xi}} + \mathbf{G}^h_s \boldsymbol{\xi} = \boldsymbol{\tau}^h_{\text{wex}}. \tag{18}$$

This equation commonly used in hydrodynamics resembles a differential equation but *it is not* because it only describes the motion in steady state for sinusiodal motion. This equation is merely a different way of describing the *frequency response function* (FRF) of the vessel from force to motion (Tick, 1959). As commented by Cummins (1962), a lot of confusion has been created by imbedding the FRF in the false time-domain model.

6. SEAKEEPING COMPUTATIONS

Most commercially available hydrodynamic codes use potential theory and the frequency domain

approach to compute the parameters in (18)—see, for example, WAMIT (2004), Fathi (2004), and Jouernee and Adegeest (2003). These codes use data of the geometry of the vessel and its loading condition (mass and load distribution). The underlying theory used depends on the speed regime of the vessel as indicated in Figure 1. These codes determine, amongst other things, the following:

- Parameters $\mathbf{M}^h_{RB}, \mathbf{A}^h(\omega, U), \mathbf{B}^h(\omega, U), \mathbf{G}^h_s$,
- Wave to Force FRF (Force FRF),
- Wave to Motion FRF (Motion FRF).

The Force FRF are considered from wave elevation to wave excitation forces, and the Motion FRF from the wave elevation to the motion components. The magnitude of the frequency response functions is commonly called *Response Amplitude Operator* (RAO) in the marine environment.

If the sea surface elevation is considered at the origin of the h-frame, we can denote the Force FRF as

$$\mathbf{F}(j\omega) = [F_1(j\omega), \ldots, F_6(j\omega)]^T. \tag{19}$$

Similarly, we denote the Motion FRF as

$$\mathbf{H}(j\omega) = [H_1(j\omega), \ldots, H_6(j\omega)]^T. \tag{20}$$

These two FRF are related via the *Force to Motion FRF*:

$$\mathbf{H}(j\omega) = \mathbf{G}(j\omega)\mathbf{F}(j\omega), \tag{21}$$

where

$$\begin{aligned}\mathbf{G}(j\omega) &= \begin{bmatrix} G_{11}(j\omega) & \cdots & G_{16}(j\omega) \\ \vdots & & \vdots \\ G_{61}(j\omega) & \cdots & G_{66}(j\omega) \end{bmatrix} \\ &= [-(\mathbf{M}^h_{RB} + \mathbf{A}^h(\omega))\omega^2 + j\omega\mathbf{B}^h(\omega) + \mathbf{G}^h_s]^{-1}\end{aligned} \tag{22}$$

We have not made it explicit, but the Force FRF depend on the encounter angle χ (the angle of the wave propagation direction relative to the heading of the vessel) and the forward speed U. The Force to Motion FRF depend only on U.

The hydrodynamic calculations are performed for a set of discrete frequencies (usually 40 or 50). For example, Figure 6 shows the added mass and potential damping in heave for a rectangular symmetric barge (8x45m) at zero forward speed. Figure 7 show the corresponding force and motion FRF for an encounter angle of 45deg (quartering seas). These coefficients were calculated with WAMIT, which is a commercial code based on 3D potential theory for marine structures at zero forward speed—see (WAMIT, 2004).

Thus, if we have access to the geometry of the hull, and the loading condition, we can use hydrodynamic computations to obtain data in 6 DOF similar to that shown in Figures 6 and 7.

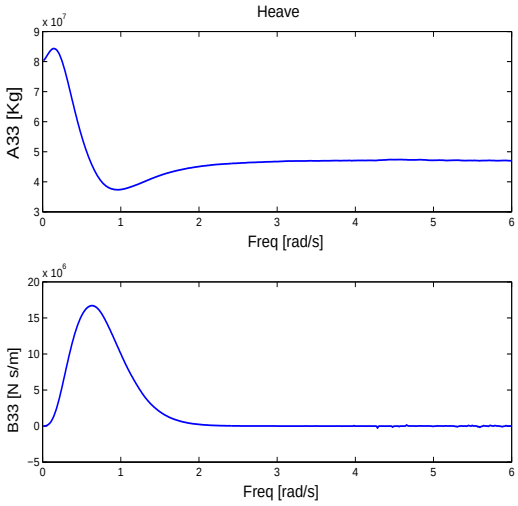

Fig. 6. Heave added mass and potential damping for a symmetric barge 8x45m at zero speed.

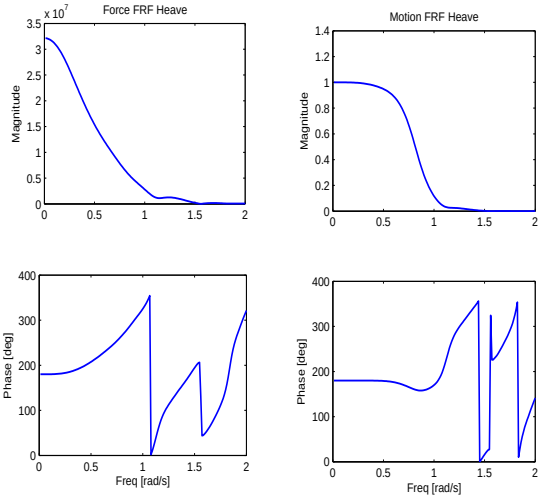

Fig. 7. Force and Motion FRF in for a symmetric barge 8x45m at zero speed.

7. LINEAR TIME-DOMAIN EQUATIONS OF MOTION

As discussed in section 5, equation (18) is not a true vector equation of motion, but a different way of writing the frequency response of the vessel. As argued by Cummins (1962), one way of seeing that this is not a true equation of motion is that if the amplitude of the sinusoidal excitation $\boldsymbol{\tau}^h_{\text{wex}}$ suddenly doubles, equation (18) does not describe the true response of the vessel.

Cummins (1962) considered the behaviour of the fluid and the ship in the time-domain *ab initio*. He made the assumption of linearity, and considered impulses in the components of motion. This resulted in a boundary value problem in which the potential was separated into two parts; one valid during the duration of the impulses and the other valid after the impulses extinguished. By express-

ing the pressure as a function of these potentials and integrating it over the wetted surface of the vessel, he obtained a vector integro-differential equation, which is known as the *Cummins Equation*:

$$[\mathbf{M}^h_{RB} + \bar{\mathbf{A}}^h]\ddot{\boldsymbol{\xi}} + \bar{\mathbf{B}}\dot{\boldsymbol{\xi}} + \int_0^t \mathbf{K}^h(t-\tau)\,\dot{\boldsymbol{\xi}}(\tau)\,d\tau + [\mathbf{G}^h_s + \mathbf{G}^h_d]\boldsymbol{\xi} = \boldsymbol{\tau}^h_{\text{exc}}. \quad (23)$$

Equation (23) reveals the structure of the linear equations of motion in the h-frame. This equation is valid for any excitation, provided the linear assumption is not violated. That is, the forces produce small displacements from a state of equilibrium.

The terms proportional to the accelerations due to the change in momentum of the fluid have constant coefficients—i.e., $\bar{\mathbf{A}}^h = \{\bar{A}_{ik}\}$ is constant, and independent of the frequency of motion and the forward speed of the vessel.

The term $\bar{\mathbf{B}}^h\dot{\boldsymbol{\xi}}$ is also frequency independent, but it depends on the steady forward speed and vanishes when the forward speed is zero.

For the case of forward speed, the pressure supporting the hull can be divided into hydrostatic and hydrodynamic pressure. Therefore, there are two restoring components: The hydrostatic one $\mathbf{G}^h_s\boldsymbol{\xi}$ and the hydrodynamic one $\mathbf{G}^h_d\boldsymbol{\xi}$, which changes with the speed due to changes in the hydrodynamic pressure. The hydrodynamic restoring terms are usually not considered for low Froude numbers: $Fn \leq 0.3$.

Due to the motion of the ship, waves are generated in the free surface. These waves will, in principle, persist at all subsequent times affecting the motion of the ship. This is know as *fluid memory effects* , and are captured in the convolution integral involving $\dot{\xi}$ and a set of *retardation functions* $\mathbf{K}^h(t-\tau)$. These functions depend on the shape of the vessel and the forward speed. This effect appears due to the free surface. For sinusoidal motions, these integrals have components in phase with the motion and 90 deg out of phase. the later components contribute to damping, whereas the components in phase with the motion can be added as frequency dependant added mass.

8. THE OGILVIE RELATIONS

Ogilvie (1964), took the Fourier transform of equation (23) and found the following relationships:

$$\begin{aligned}\mathbf{A}^h(\omega) &= \bar{\mathbf{A}}^h - \frac{1}{\omega}\int_0^\infty \mathbf{K}^h(t)\,\sin(\omega\tau)\,d\tau,\\ \mathbf{B}^h(\omega) &= \bar{\mathbf{B}}^h + \int_0^\infty \mathbf{K}^h(t)\,\cos(\omega\tau)\,d\tau.\end{aligned} \quad (24)$$

By taking the limit as $\omega \to \infty$ in (24), it follows from the Riemann-Lebesgue Lemma that

$$\begin{aligned}\bar{\mathbf{A}}^h &= \lim_{\omega\to\infty}\mathbf{A}^h(\omega) = \mathbf{A}^h(\infty),\\ \bar{\mathbf{B}}^h &= \lim_{\omega\to\infty}\mathbf{B}^h(\omega) = \mathbf{B}^h(\infty).\end{aligned} \quad (25)$$

These infinity values (25) can be calculated by solving a special boundary value problem with the condition that the potential vanishes on the free surface (Faltinsen, 1990).

By taking the inverse of the Fourier cosine transform in (24), we obtain

$$\mathbf{K}^h(t) = \frac{2}{\pi}\int_0^\infty [\mathbf{B}^h(\omega) - \mathbf{B}^h(\infty)]\cos(\omega t)d\omega. \quad (26)$$

This expression can be used to compute and approximation of the retardation functions from knowledge of the damping coefficients for frequencies up to a high value. For example, Figure 8 shows the retardation functions for diagonal elements of the matrix $\mathbf{K}^h(t-\tau)$ for a symmetrical barge at zero speed, which were computed using (26).

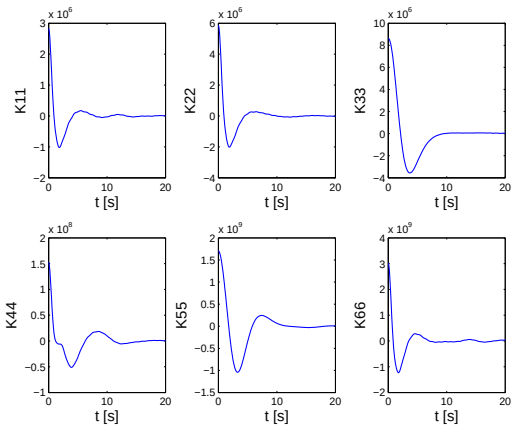

Fig. 8. Retardation functions for a symmetric barge 8x45m at zero speed.

Figure 9 shows a block diagram representative of a linear time-domain model. In this model, the true structure of the equations of motion can be appreciated.

9. PROPERTIES OF THE RETARDATION FUNCTIONS

9.1 Time-domain properties of the retardation functions

- **Asymptotic value for** $t = 0$: It follows from (26), that

$$\lim_{t\to 0}\mathbf{K}^h(t) \neq \mathbf{0} < \infty. \quad (27)$$

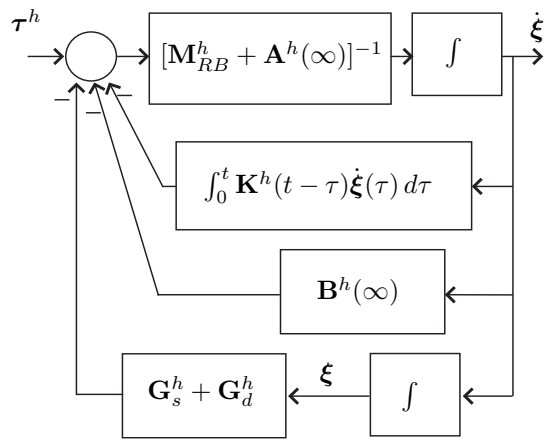

Fig. 9. Block diagram representation of the Cummins Equation

- **Asymptotic for** $t \to \infty$:

$$\lim_{t\to\infty} \mathbf{K}^h(t) = \mathbf{0}, \tag{28}$$

which follows from the application of the Riemann-Lebesgue Lemma to (26) and the fact that $\int_0^\infty [\mathbf{B}^h(\omega) - \mathbf{B}^h(\infty)]d\omega$ is absolutely convergent—this is the result for $t = 0$ above. This result for infinite time can alternatively be obtained by considering that for the convolution representation to exists the system needs to be BIBO stable; and can only happen if the impulse response of the system converges to zero as time goes to infinity.

9.2 Frequency-domain properties of the retardation functions

The frequency response of the convolutions are given by

$$\begin{aligned}\mathbf{K}^h(j\omega) &= \int_0^\infty \mathbf{K}^h(t)\, e^{-j\omega\tau} d\tau \\ &= \mathbf{B}^h(\omega) - \mathbf{B}^h(\infty) + j\omega[\mathbf{A}^h(\omega) - \mathbf{A}^h(\infty)].\end{aligned} \tag{29}$$

This follows from multiplying the first equation in (24) by $j\omega$, and adding it to the second. From this,

- **Asymptotic for** $\omega \to 0$:

$$\lim_{\omega\to 0} \mathbf{K}^h(j\omega) = \mathbf{0}. \tag{30}$$

- **Asymptotic for** $\omega \to \infty$:

$$\lim_{\omega\to\infty} \mathbf{K}^h(j\omega) = \mathbf{0}. \tag{31}$$

  This follows from (24) and the Riemman-Lebesgue Lemma.
- **Relative degree**: *The relative degree of* $K^h_{ik}(s)$ *is 1.* This follows from (27), and the application of the initial value theorem of the Laplace transform.
- **Passivity**: Passivity is an important property for systems which establish that the system is dissipative. For a LTI system, passivity is equivalent to positive realness (PR) of the transfer function. In the scalar case, all rational PR functions have necessarily relative degree one and are stable. Therefore, input-output mapping of the convolution terms is passive—see. for example, Damaren (2000) for further details.

10. EQUIVALENT REPRESENTATIONS FOR SIMULATION AND CONTROL DESIGN

Although the model (23) is a time-domain model, the convolution term makes it awkward for analysis and design of control systems. This is, can be easily solved in two different ways. The first one consists of replacing the convolution terms by equivalent transfer functions or state-space representations. The second approach consists of replacing the model from force to motion by equivalent transfer functions or state-space representation (Perez and Lande, 2006). In this paper, we will focuss only on the first approach.

The equivalent representation of the convolution terms by a state space realization has been reported in the literature by different authors using different methods. For example, Yu and Falnes (1995) (1998) obtain a continuous-time state-space model from samples of the impulse response calculated from (26). The method proposed uses a companion form for the realization $(\mathbf{A}_c, \mathbf{B}_c, \mathbf{C}_c)$ for each entry of the convolution matrix. Once the order of the scalar system chosen (by inspection of the plot of $K^h_{ik}(t)$), the parameter estimation problem is posed as a non-linear LS-problem:

$$\begin{aligned}\boldsymbol{\theta}^\star = \arg\min_{\boldsymbol{\theta}} \\ \sum_j W_j |K^h_{ik}(t_j) - \mathbf{C}_c(\boldsymbol{\theta})\, e^{\mathbf{A}_c(\boldsymbol{\theta})\, t_j} \mathbf{B}_c(\boldsymbol{\theta})|^2,\end{aligned}$$

This problem can then be solved using Gauss-Newton methods. The weighting function W_j needs to be chosen carefully for the results to be accurate—see Yu and Falnes (1998) for details.

Kristansen and Egeland (2003) and Kristiansen *et al.* (2005) use realization theory instead, and employ an algorithm that estimates the state-space realization of a discrete time-model based on the sampled impulse response. In this approach, the authors use the function `imp2ss` from the robust control toolbox in MATLAB, which is based on the algorithm of Kung (1978). This algorithm estimates the order of the model and the matrices from a singular value decomposition of the Hankel matrix of the Markov parameters (impulse response).

Apart from the references mentioned above, the rest of the literature seemed to have favored the frequency-domain approach to fit a transfer function to the frequency response of the convolution or a related transfer function. For example, Damaren (2000) and McCabe *et al.* (2005) consider the case of zero forward speed and fit transfer functions to the frequency response of the convolutions. That is, given the frequency responses $K^h_{ik}(\omega)$ (29), we seek a rational approximation:

$$\hat{K}^h_{ik}(s) = \frac{P(s)}{Q(s)} = \frac{p_m s^m + p_{m-1}s^{m-1} + \cdots + p_0}{s^n + q_{n-1}s^{n-1} + \cdots + q_0}$$

where $P(s)$ and $Q(s)$ are polynomials of appropriate dimensions. From the results of Section 9, it follows that the rational approximation must satisfy the following:

- It has a zero at s=0,
- It has relative degree 1.

Thus, we can fusther specify the structure of the model as

$$\hat{K}^h_{ik}(s) = \frac{s^l P'(s)}{Q(s)}.$$

In general, $l = 1$. This is easy to check by plotting the Bode diagram of $K_{ik}(\omega)$ and looking at the asymptotic slope of the magnitude and the phase at low frequencies. Assuming $l = 1$, the degree of the denominator should be $n = m + 2$. In other words, if $l = 1$, $deg(P') = deg(Q) - 2$, and the lowest possible order approximation consistent with the properties of the convolution results in

$$n = 2, \qquad l = 1, \qquad m = 0.$$

Having established the structure of the rational approximation, we need to estimate the parameters:

$$\boldsymbol{\theta} = [p_m, ..., p_0, q_{n-1}, ..., q_0,]^T.$$

The estimation problem results in the following optimization problem:

$$\boldsymbol{\theta}^\star = \arg\min_{\boldsymbol{\theta}} \sum_l W_l \left| K^h_{ik}(\omega_l) - \frac{P(j\omega_l, \theta)}{Q(j\omega_l, \theta)} \right|^2. \quad (32)$$

This is a NL LS-problem that can be solved, for example, using the function `lsqnonlin` of the optimization toolbox of Matlab. Alternatively a linearized version or Levi Method (Levi, 1959) can be attempted, which results in a linear LS problem. The function `invfrecs` of the signal processing toolbox in MATLAB implements the Levi method. This function also has the option of solving the NL problem via Gauss-Newton using the estimate of the linear problem a initial condition. For a further discussion about the application of this methods see (Perez and Lande, 2006).

For example, Figure 10 shows the fitting of the convolution term for heave $K^h_{33}(\omega)$ and its estimate $\hat{K}^h_{33}(\omega)$ of a barge example. These results were obtained from NL LS method in the frequency-domain using `invfrecs`. The approximation is of 4th-order.

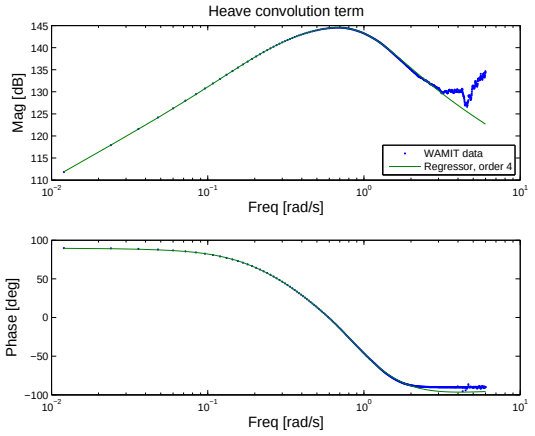

Fig. 10. Convolution term FRF $K^h_{33}(\omega)$ and its estimate $\hat{K}^h_{33}(\omega)$.

After finding the linear system approximations $\hat{K}^h_{ik}(s)$ to the convolution terms, these can be converted to state space realizations. Then, by combining all state-space models into an augmented model, we can express the Cummins equation (23) as

$$\begin{aligned} [\mathbf{M}^h_{RB} + \mathbf{A}(\infty)]\ddot{\boldsymbol{\xi}} + \mathbf{B}(\infty)\dot{\boldsymbol{\xi}} + \boldsymbol{\mu}^h + [\mathbf{G}^h_s + \mathbf{G}^h_d]\boldsymbol{\xi} &= \boldsymbol{\tau}^h_{\text{exc}}, \\ \dot{\mathbf{x}} &= \mathbf{A}^h_r \mathbf{x} + \mathbf{B}^h_r \dot{\boldsymbol{\xi}} \\ \boldsymbol{\mu}^h &= \mathbf{C}^h_r \mathbf{x}. \end{aligned} \quad (33)$$

11. CONVERTING THE MODEL TO BODY-FIXED COORDINATES

We have seen that the Cummins equation is a LTI vector equation of motion. This equation is given in terms of seakeeping or perturbation coordinates. Therefore, in order to have model for control design it is necessary to express this model in terms of body-fixed coordinates.

Using the small angle kinematic transformations between unified and seakeeping coordinates (see Appendix)

$$\begin{aligned} \dot{\boldsymbol{\xi}} &= \mathbf{J}^{-1}[\delta\boldsymbol{\nu} + \mathbf{L}U\delta\boldsymbol{\eta}], \\ \ddot{\boldsymbol{\xi}} &= \mathbf{J}^{-1}[\delta\dot{\boldsymbol{\nu}} + \mathbf{L}U\delta\dot{\boldsymbol{\nu}}], \end{aligned} \quad (34)$$

we can express (23) as

$$\begin{aligned} [\mathbf{M}^h_{RB} + \mathbf{A}(\infty)]\mathbf{J}^{-1}[\delta\dot{\boldsymbol{\nu}} + \mathbf{L}U\delta\boldsymbol{\nu}] \\ + \mathbf{B}(\infty)\mathbf{J}^{-1}[\delta\boldsymbol{\nu} + \mathbf{L}U\delta\boldsymbol{\eta}] \\ + \int_0^t \mathbf{K}^h(t-\tau)\,\mathbf{J}^{-1}[\delta\boldsymbol{\nu}(\tau) + \mathbf{L}U\delta\boldsymbol{\eta}(\tau)]\,d\tau \\ + [\mathbf{G}^h_s + \mathbf{G}^h_d]\boldsymbol{\xi} = \boldsymbol{\tau}^h_{\text{exc}}. \end{aligned} \quad (35)$$

By multiplying the above equation by $\mathbf{J}^{-T}$, we obtain

$$\begin{aligned}\mathbf{M}\delta\dot{\boldsymbol{\nu}} + [\mathbf{C}_{RB} + \mathbf{C}_A]\delta\boldsymbol{\nu} + \mathbf{D}\delta\boldsymbol{\nu} \\ + \int_0^t \mathbf{K}(t-\tau)\left[\delta\boldsymbol{\nu}(\tau) + \mathbf{L}U\delta\boldsymbol{\eta}(\tau)\right] d\tau \\ + \mathbf{G}\delta\boldsymbol{\eta} = \boldsymbol{\tau}^b_{\text{wex}}, \quad (36)\end{aligned}$$

where

$$\begin{aligned}\mathbf{M} &= \mathbf{J}^{-T}[\mathbf{M}^h_{RB} + \mathbf{A}(\infty)]\mathbf{J}^{-1}, \\ \mathbf{C}_{RB} &= \mathbf{J}^{-T}\mathbf{M}^h_{RB}\mathbf{J}^{-1}\mathbf{L}U, \\ \mathbf{C}_A &= \mathbf{J}^{-T}\mathbf{A}(\infty)\mathbf{J}^{-1}\mathbf{L}U, \\ \mathbf{D} &= \mathbf{J}^{-T}\mathbf{B}(\infty)\mathbf{J}^{-1}, \\ \mathbf{K}(t) &= \mathbf{J}^{-T}\mathbf{K}^h(t)\,\mathbf{J}^{-1}, \\ \mathbf{G} &= U\mathbf{D}\mathbf{L} + \mathbf{J}^{-T}[\mathbf{G}^h_s + \mathbf{G}^h_d], \\ \boldsymbol{\tau}^b_{\text{wex}} &= \mathbf{J}^{-T}\boldsymbol{\tau}^h_{\text{wex}}.\end{aligned} \quad (37)$$

In this model, we have the total Coriolis matrices $\mathbf{C}_{RB}$ and $\mathbf{C}_A$ due to rigid body and added mass. Equation (36) is the Cummins equation in the b-frame. Note also that in this simplified representation, $\delta\boldsymbol{\eta}$ is assumed to be negligible only for the kinematic transformation, which results in a constant matrix $\mathbf{J}$—see Appendix A.

In Fossen (2005) and Perez (2005), a different approach was used to obtain (36). The frequency domain model was transformed to the b-frame first, and then the frequency dependant terms were replaced by a convolution. As a result, the expression in Fossen (2005) and Perez (2005) is of the same form as (36), but the elements in (37) have a different form.

Note that because of the type of transformation in (37) for $\mathbf{K}(t)$, the properties described in Section 9 are maintained. Therefore, after performing identification to replace the convolution by an equivalent linear system using any of the methods given in Section 10, equation (36) can be expressed as

$$\begin{aligned}\mathbf{M}\delta\dot{\boldsymbol{\nu}} + [\mathbf{C}_{RB} + \mathbf{C}_A]\delta\boldsymbol{\nu} + \mathbf{D}\delta\boldsymbol{\nu} \\ + \boldsymbol{\mu} + \mathbf{G}\delta\boldsymbol{\eta} = \boldsymbol{\tau}^b_{\text{wex}} + \delta\boldsymbol{\tau}^b, \quad (38)\end{aligned}$$

$$\begin{aligned}\dot{\mathbf{x}} &= \mathbf{A}_r\mathbf{x} + \mathbf{B}_r[\delta\boldsymbol{\nu} + \mathbf{L}U\delta\boldsymbol{\eta}] \\ \boldsymbol{\mu} &= \mathbf{C}_r\mathbf{x},\end{aligned}$$

where the state-space realization $\mathbf{A}_r, \mathbf{B}_r, \mathbf{C}_r$ is obtained by grouping state-space realizations. If the identification is performed for $\mathbf{K}^h(j\omega)$, then the following relations can be used to transform the resulting state-space model:

$$\begin{aligned}\mathbf{A}_r &= \mathbf{A}^h_r, \\ \mathbf{B}_r &= \mathbf{B}^h_r\mathbf{J}^{-1} \\ \mathbf{C}_r &= \mathbf{J}^{-T}\mathbf{C}^h_r.\end{aligned}$$

Finally, by substituting the perturbation terms in (38) and adding the kinematic transformation (4), we obtain

$$\begin{aligned}\mathbf{M}\dot{\boldsymbol{\nu}} + \mathbf{C}\boldsymbol{\nu} + \mathbf{D}\boldsymbol{\nu} + \mathbf{C}_r\mathbf{x} + \mathbf{G}\boldsymbol{\eta} = \boldsymbol{\tau}^b_{\text{wex}} + \boldsymbol{\tau}^b, \\ \dot{\mathbf{x}} = \mathbf{A}_r\mathbf{x} + \mathbf{B}_r[(\boldsymbol{\nu} - \bar{\boldsymbol{\nu}}) + \mathbf{L}U\boldsymbol{\eta}] \\ \dot{\boldsymbol{\eta}} = \mathbf{J}^n_b(\overline{\boldsymbol{\Theta}}_{nb})\boldsymbol{\nu}.\end{aligned} \quad (39)$$

This expression is similar to that given in (Fossen, 2005) and Perez (2005).

12. ADDING VISCOUS EFFECTS

The model (39) was derived from seakeeping data based on o potential theory. Therefore, the model lacks viscous damping. This damping can be added to the time-domain model, and the coefficients estimated based on experimental data. That is, another term

$$\mathbf{D}_v(\boldsymbol{\nu})\boldsymbol{\nu} = \mathbf{D}_{vl}\boldsymbol{\nu} + \mathbf{D}_{vnl}\boldsymbol{\nu}|\boldsymbol{\nu}|$$

can be added to the left-hand side of the top equation in (39). This terms include linear skin friction, viscous roll damping and cross-flow drag. Alternatively, a linear viscous damping can be added to the frequency-domain model:

$$\mathbf{B}_{\text{tot}}(\omega) = \mathbf{B}(\omega) + \mathbf{B}_v(\omega),$$

and then use the total damping to compute the convolution for the time domain model. This approached was proposed by Bailey *et al.* (1997) and Fossen (2005). However, Since $\mathbf{B}_v(\omega)$ can be approximated with a constant matrix, it may be preferable to add the viscous effects in the time domain. This is further discussed in Ross *et al.* (2006).

13. WAVE EXCITATION FORCES

The wave excitation forces are disturbances. These can be modeled as a time series based on the wave spectrum $\mathrm{S}_{\zeta\zeta}(\omega, \chi)$ and the force FRF $F_i(\omega, \chi)$):

$$\tau^h_{wex,i}(t) = \sum_{n=1}^{N}\sum_{m=1}^{M} \bar{\tau}_{inm}\cos\left[\omega_{nm}t + \varphi_{imn}\right],$$

for $i = 1, \ldots, 6$, with

$$\varphi_{imn} = \arg F_i(\omega^*_n, \chi^*_m) + \varepsilon_n$$

$$\bar{\tau}_{inm} = \sqrt{2|F_i(\omega^*_n, \chi^*_m)|^2 \mathrm{S}_{\zeta\zeta}(\omega^*_n, \chi^*_m)\Delta\chi\Delta\omega},$$

where H_i are the force FRF of the vessel, and ω^*_n and χ^*_m are chosen randomly in the intervals

$$\left[\omega_n - \frac{\Delta\omega}{2}, \omega_n + \frac{\Delta\omega}{2}\right], \quad \left[\chi_m - \frac{\Delta\chi}{2}, \chi_m + \frac{\Delta\chi}{2}\right].$$

For further details see Perez (2005).

14. CONCLUSION

In this paper, we have discussed the use of seakeeping data computed from standard hydrodynamic codes to obtain time-domain models for simulation and control design. We have revisited the classical frequency domain approach used in in hydrodynamics together with the resulting linear time-domain model. The latter model is a vector integro differential equation that is not convenient for analysis and design of control systems. Therefore, by using system identification one can approximate the convolution terms by the response of linear systems. By combining these linear systems with the rest of the model we obtain a model suitable for analysis and design in body-fixed coordinates. We further discussed the need to add viscous effects.

REFERENCES

Abkowitz, M.A. (1964). Lectures on ship hydrodynamics—steering and manoeuvrability. Technical Report Rep. No. Hy-5. Hydro og Aerodynamisk Laboratorium, Lyngby, Denmark.

Bailey, P.A., W.G. Price and P. Temarel (1997). A unified mathematical model describing the manoeuvring of a ship in s seaway. *Transactions The Royal Institution of Naval Architects–RINA* **140**, 131–149.

Beck, R.F. and A.M. Reed (2001). Modern computational methods for ships in a seaway. *SNAME Transactions* **109**, 1–51.

Clarke, D. (2003). The foundations of steering and manoeuvring. In: *6th IFAC Conference on Manoeuvring and Control of Marine Craft MCMC'03, Girona, Spain*. pp. –.

Cummins, W.E. (1962). The impulse response function and ship motion. Technical Report 1661. David Taylor Model Basin–DTNSRDC.

Damaren, C.J. (2000). Time-domain floating body dynamics by rational approximations of the radiation impedance and diffraction mapping. *Ocean Engineering* **27**, 687–705.

Faltinsen, O.M. (1990). *Sea Loads on Ships and Offshore Structures*. Cambridge University Press.

Faltinsen, O.M. (2005). *Hydrodynamic of High-speed Marine Vehicles*. Cambridge University Press.

Fathi, D. (2004). *ShipX Vessel Responses (VERES)*. Marintek AS Trondheim. http://www.marintek.sintef.no/.

Fossen, T.I. (1994). *Guidance and Control of Ocean Marine Vehicles*. John Wiley and Sons Ltd. New York.

Fossen, T.I. (2002). *Marine Control Systems: Guidance, Navigation and Control of Ships, Rigs and Underwater Vehicles*. Marine Cybernetics, Trondheim.

Fossen, T.I. (2005). A nonlinear unified state-space model for ship maneuvreing and control in a seaway. In: *International Journal of Bifurcation and Chaos*. Vol. 15. pp. 2717–2746.

Ikeda, Y., K. Komatsu, Y. Himeno and N. Tanaka (1976). On roll damping force of ship: Effects of friction of hull and normal force of bilge keels. *J. Kansai Society of Naval Architects* **142**, 54–66.

Jouernee, J.M.J. and L.J.M. Adegeest (2003). *Theoretical Manual of Strip Theory Program* SEAWAY *for Windows*. TU Delft, Delft University of Technology. www.ocp.tudelft.nl/mt/journee.

Kristansen, E. and O. Egeland (2003). Frequency dependent added mass in models for controller design for wave motion ship damping.. In: *6th IFAC Conference on Manoeuvring and Control of Marine Craft MCMC'03, Girona, Spain.*

Kristiansen, E., A. Hjuslstad and O. Egeland (2005). State-space representation of radiation forces in time-domain vessel models. *Ocean Engineering* **32**, 2195–2216.

Kung, S.Y. (1978). A new identification and model reduction algorithm via singular value decompositions. *Twelth Asilomar Conf. on Circuits, Systems and Computers* pp. 705–714.

Levi, E.C. (1959). Complex-curve fitting. *IRE Trans. on Automatic Control*.

Lloyd, A.R.J.M. (1998). *Seakeeping: Ship Behaviour in Rough Weather*. A.R.J.M. Lloyd, 26 Spithead Av., Gosport, Hampshire, UK.

McCabe, A.P., A. Bradshaw and M.B. Widden (2005). A time-doamin model of a floating body usign transforms. In: *Proc. of 6th European Wave and Tidal energy Conference*. University of Strathclyde, Glasgow, U.K.

Newman, J.N. (1977). *Marine Hydrodynamics*. MIT Press.

Norrbin, N.H. (1970). Theory and observation on the use of a mathematical model for ship manoeuvring in deep and confined waters. *8th Symposium on Naval Hydrodynamics, USA*.

Ogilvie, T. (1964). Recent progress towards the understanding and prediction of ship motions. In: *6th Symposium on Naval Hydrodynamics*.

Perez, T. (2005). *Ship Motion Cotnrol: Course Keeping and Roll Reduction using rudder and fins*. Advances in Industrial Control. Springer-Verlag, London.

Perez, T, A.J. Sorensen and M. Blanke (2006). Marine vessel models in changing operational conditionsa tutorial. In: *Proceedings of 14th IFAC workshop on system identification. Newcastle, Australia*.

Perez, T. and Ø. Lande (2006). A frequency-domain approach to modelling and identification of the force to motion vessel response. In: *Proc. of 7th IFAC Conference on Manoeuvring and Control of marine Craft, Lisbon, Portugal*.

Perez, T., T.I. Fossen and A.J. Sørensen (2004). A discussion about seakeeping and manoeuvring models for surface vessels. Technical report MSS-TR-001. Centre for Ships and Ocean Structures (CESOS), Norwegian University of Science and Technology NTNU, Trondheim, Norway. Available at http://www.cesos.ntnu.no/mss/.

Ross, A., T. Perez and T.I. Fossen (2006). Clarification of the low-frequency modelling concept for marine craft. In: *Proc. 7th IFAC Conference on Manoeuvring and Control of Marine Craft, Lisbon, Portugal*.

SNAME (1950). Nomenclature for treating the motion of a submerged body through a fluid. Technical Report Bulletin 1-5. Society of Naval Architects and Marine Engineers, New York, USA.

WAMIT (2004). WAMIT *User Manual*. www.wamit.com.

Tick, L.J. (1959). Differential equations with frequency-dependent coefficients. *ship Research* **2**(2), 45–46.

Yu, Z. and J. Falnes (1995). Spate-space modelling of a vertical cylinder in heave. *Applied Ocean Research* **17**, 265–275.

Yu, Z. and J. Falnes (1998). State-space modelling of dynamic systems in ocean engineering. *Journal of hydrodynamics, China Ocean Press* pp. 1–17.

Appendix A. TRANSFORMATIONS BETWEEN UNIFIED AND SEAKEEPING COORDINATES

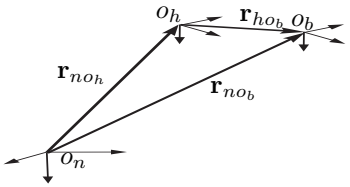

Fig. A.1. Relative position of frames.

By considering the relative position of the frames shown in Figure A.1, taking the time derivatives and expressing the vectors in a the b-frame, we arrive to the following linear velocity transformation:

$$\mathbf{v}^b_{no_b} = \mathbf{R}^b_n \mathbf{v}^n_{no_h} + \mathbf{R}^b_h [\mathbf{I}_{3\times 3} \quad \mathbf{S}^T(\mathbf{r}^h_{so_b})] \dot{\boldsymbol{\xi}} + \mathbf{R}^b_n \mathbf{S}(\boldsymbol{\omega}^n_{nh}) \mathbf{R}^n_h \mathbf{r}^h_{ho_b}, \quad \text{(A.1)}$$

where the *skew-symmetric operator* $\mathbf{S}(\cdot)$ defined as:

$$\mathbf{S} : R^3 \mapsto R^{3\times 3}, \mathbf{S}(\mathbf{x}) = \begin{bmatrix} 0 & -x_3 & x_2 \\ x_3 & 0 & -x_1 \\ -x_2 & x_1 & 0 \end{bmatrix}, \quad \text{(A.2)}$$

with $\mathbf{x} = [x_1, x_2, x_3]^T$, and $\mathbf{S} = -\mathbf{S}^T$.

Because the h-frame is considered inertial, then $\mathbf{v}^n_{no_h} = \bar{\mathbf{v}}^n_{no_h}$ constant, and $\boldsymbol{\omega}^n_{nh} \approx 0$.

Then, by combing (A.1) with the angular velocity transformation, it follows that the kinematic transformation between the h- and the b-frame is

$$\boldsymbol{\nu} = \mathbf{J}^b_h(\boldsymbol{\Theta}_{hb}, \mathbf{r}^h_{so_b}) \dot{\boldsymbol{\xi}} + \begin{bmatrix} \mathbf{R}^b_n(\boldsymbol{\Theta}_{nb}) \\ \mathbf{0}_{3\times 3} \end{bmatrix} \bar{\mathbf{v}}^n_{no_h}, \quad \text{(A.3)}$$

with

$$\mathbf{J}^b_h(\boldsymbol{\Theta}_{hb}, \mathbf{r}^h_{so_b}) \triangleq \begin{bmatrix} \mathbf{R}^b_h(\boldsymbol{\Theta}_{hb}) & \mathbf{R}^b_h(\boldsymbol{\Theta}_{hb}) \mathbf{S}^T(\mathbf{r}^h_{so_b}) \\ \mathbf{0}_{3\times 3} & \mathbf{T}_{\boldsymbol{\Theta}}(\boldsymbol{\Theta}_{hb})^{-1} \end{bmatrix}. \quad \text{(A.4)}$$

In (A.4) the matrices $\mathbf{R}^b_h(\boldsymbol{\Theta}_{hb})$ and $\mathbf{T}_{\boldsymbol{\Theta}}(\boldsymbol{\Theta}_{hb})$ are defined as in (6) and (7) using the Euler angles that take the h-frame into the orientation of the b-frame—*c.f.* (10).

Note that the transformation (A.3) accounts for the fact that the position of body-fixed frame b may be chosen different from the position of the s-frame (which coincides with the h-frame when the vessel sails in the equilibrium condition). This is a desirable feature for control design purposes because we can position the origin of the b-frame in a convenient location for the particular control problem considered.

If we separate the Euler angles into

$$\psi = \overline{\psi} + \delta\psi, \quad \phi = \overline{\phi} + \delta\phi, \quad \theta = \overline{\theta} + \delta\theta. \quad \text{(A.5)}$$

in which, as already mentioned, we usually consider $\overline{\phi} = \overline{\theta} = 0$, then for small perturbation angles we obtain the following approximation for (A.3):

$$\delta\boldsymbol{\nu} \approx \mathbf{J}\dot{\boldsymbol{\xi}} - \mathbf{L}U\boldsymbol{\xi}. \quad \text{(A.6)}$$

where

$$\mathbf{J} \triangleq \begin{bmatrix} \mathbf{I}_{3\times 3} & \mathbf{S}^T(\mathbf{r}^s_{so_b}) \\ \mathbf{0}_{3\times 3} & \mathbf{I}_{3\times 3} \end{bmatrix} = \mathbf{J}^b_h(\boldsymbol{\Theta}_{hb}, \mathbf{r}^s_{so_b})\big|_{\boldsymbol{\Theta}_{hb}=\mathbf{0}}, \quad \text{(A.7)}$$

and

$$\mathbf{L} \triangleq \begin{bmatrix} 0 & \cdots & & & 0 \\ 0 & \cdots & 0 & 0 & 1 \\ 0 & \cdots & 0 & -1 & 0 \\ 0 & \cdots & & & 0 \\ \vdots & \ddots & & & \vdots \\ 0 & \cdots & & & 0 \end{bmatrix}. \quad \text{(A.8)}$$

The inverse kinematic transformation of (A.6) is of the form

$$\dot{\boldsymbol{\xi}} \approx \mathbf{J}^{-1}[\delta\boldsymbol{\nu} + \mathbf{L}U\delta\boldsymbol{\eta}], \quad \text{(A.9)}$$

where

$$\mathbf{J}^{-1} = \begin{bmatrix} \mathbf{I}_{3\times 3} & \mathbf{S}(\mathbf{r}^s_{so_b}) \\ \mathbf{0}_{3\times 3} & \mathbf{I}_{3\times 3} \end{bmatrix}. \quad \text{(A.10)}$$